Near-Minimum Time, Closed-Loop Slewing of Flexible Spacecraft

R. M Byers,* S. R. Vadali,† and J. L. Junkins‡
Texas A&M University, College Station, Texas

The near-minimum time single-axis slewing of a flexible spacecraft with simultaneous suppression of vibration of elastic modes is considered. The hyperbolic tangent (tanh) function is used as a smooth approximation to the discontinuous sgn function occurring in the rigid body "bang-bang" control. Variable structure control concepts are used to identify the necessary characteristics of the control switching line. Simulations of the rest-to-rest and tracking maneuvers indicate that the elastic energy can be reduced by several orders of magnitude with only a modest increase in the maneuver time.

Introduction

MANY future large space structures, due to mass constraints, will be flexible. For the purpose of analysis these systems can be modeled with a large number of modes of vibration. For certain applications, it will be desirable that such a spacecraft be able to slew as rapidly as possible, within the operating limits of the control actuators. The problem of control design for rotational maneuver and vibration suppression of flexible spacecraft has been addressed extensively.[1-10] Optimal control theory can be applied to enforce quiescent terminal conditions on the flexible modes, usually by applying a quadratic cost function that weights the control rates and the states. The order of the system model grows rapidly as the number of flexible modes to be controlled is increased, making it impractical to attempt to control more than a few flexible modes. Furthermore, there is no rigorous means by which control magnitude constraints may be enforced. Although a feedback method such as the linear quadratic regulator (LQR) with terminal constraints[9-11] is attractive because it can enforce quiescent conditions on the elastic modes, its computational complexity is burdensome.

The optimal control solution to the minimum time, single-axis, rotational maneuver problem for a rigid body gives a control scheme characterized by saturation of the control throughout the maneuver with at most one control switch that is instantaneous (bang-bang). Although not exactly achievable in physical systems, and even though the trajectories are extremely sensitive to variations in spacecraft parameters, this control law has wide application for rigid systems using on-off thrusters. When rigorously applied to flexible systems, however, the result is typically multiple control switches and excessive excitation of the flexible modes of vibration. Previous investigations of the near-time optimal maneuver for flexible systems[7,8] are open-loop designs requiring extensive computational effort. An alternative is to compute the required parameters for a number of initial conditions off-line and use table lookup and interpolation for a particular maneuver. This may involve excessive storage. We start with the assumption that the minimum time solution for a rigid spacecraft can serve as an initial approximation to the near-minimum time solution for a flexible structure. In other words, we expect that near-minimum times can be achieved by limiting the number of control switches to one, and vibration suppression can be achieved by torque smoothing. Singh et al.[7] observe quantitatively that the difference between the minimum time for a rigid body and the actual time required for a flexible spacecraft is small for large-angle maneuvers of systems of low flexibility and small available control torques.

To avoid exciting the flexible modes of vibration, the discontinuous sgn function associated with the minimum time solution for a rigid body is approximated by the hyperbolic tangent (tanh) function. The parabolic switching function associated with the rigid-body control is replaced by one that, also using the hyperbolic tangent function, exploits the symmetry of the rigid-body state trajectory.

The resulting control logic is a computationally simple feedback design that causes the flexible system to come very close to the desired orientation (coarse maneuver) and corrects any residual error in a fine-pointing mode using very small control inputs. A major feature of this control design is that only the rigid-body components of the state vector must be considered by the control. This approach has been adapted for a multiple-body/multiple-actuator system.

System Model and Equations of Motion

A generic flexible spacecraft is used for analysis (Fig. 1a). It consists of a rigid hub with four cantilevered flexible appendages. Continuous control torque is assumed to be provided by a single momentum exchange actuator in the central hub. Internal actuator dynamics are ignored. Only small antisymmetric deformations (Fig. 1b) in the plane normal to the axis of rotation are assumed. Damping is assumed to be negligible and is ignored.

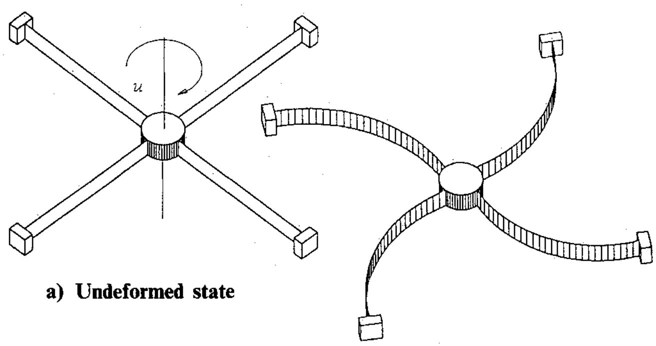

a) Undeformed state

b) Antisymmetric deformations

Fig. 1 Flexible spacecraft model.

Received June 7, 1988; revision received Aug. 24, 1988.

*Graduate Student, Department of Aerospace Engineering. Student Member AIAA.

†Assistant Professor, Department of Aerospace Engineering. Member AIAA.

‡TEES Chair Professor, Department of Aerospace Engineering. Fellow AIAA.

The dynamics of such a system may be modeled by the second-order matrix equation:

$$M\ddot{q} + Kq = Vu \tag{1}$$

where q is the $(n \times 1)$ vector of the generalized displacements of the configuration, M the $(n \times n)$ mass matrix, K the $(n \times n)$ stiffness matrix, and V the $((n \times 1)$ control influence matrix.

Unfortunately, these n equations are coupled and not in a convenient form for analysis. They can be decoupled by transforming from generalized coordinates to modal coordinates using the transformation

$$q = \Phi\eta \tag{2}$$

where Φ is the $n \times n$ matrix of normalized eigenvectors. This yields the equations of motion

$$\ddot{\eta} + \Lambda\eta = V'u \tag{3}$$

where Λ is the diagonal matrix of the system's eigenvalues, and $V' = \Phi^T V$. Since $\lambda_1 = 0$, $\eta_1 = \theta$, where θ is the spacecraft's rigid-body mode coordinate in physical space.

These equations may be further reduced to a set of $2n$ first-order differential equations. By defining the $(2n)$ vector

$$z = \begin{pmatrix} \eta \\ \dot{\eta} \end{pmatrix} \tag{4}$$

the state-space formulation can be expressed as

$$\dot{z} = Az + Bu$$

where

$$A = \begin{pmatrix} 0 & I \\ -\Lambda & 0 \end{pmatrix}, \qquad B = \begin{pmatrix} 0 \\ V' \end{pmatrix} \tag{5}$$

Numerical integration by fourth-order Runge-Kutta method was used on this system to analyze the first seven modes of the generic spacecraft.

Rigid-Body Minimum Time Optimal Control Solution

Consider a system with only a rigid-body mode with bounded control such that

$$\begin{aligned} I\ddot{\theta} &= u, & |u| &\le u_0 \\ \theta(0) &= \theta_0, & \dot{\theta}(0) &= \dot{\theta}_0 \\ \theta(t_f) &= 0, & \dot{\theta}(t_f) &= 0 \end{aligned} \tag{6}$$

where I is the moment of inertia, $\theta(t)$ the angular displacement, and u the magnitude of the control. The closed-loop solution to the rotational maneuver problem is well known[11,12]:

$$u = -u_0 \operatorname{sgn}(s) \tag{7}$$

$$s = \begin{cases} \theta(t) + I\dot{\theta}(t)|\dot{\theta}(t)|/2u_0, & 0 \le t \le t_1, \quad t_1 = \text{switch time} \\ \dot{\theta}(t), & t_1 < t \le t_f \end{cases} \tag{8}$$

It is clear that the origin of the state space can be reached from any initial condition with a maximum of one control switch at some time $t = t_1$ by initially applying $\pm u_0$ as appropriate to intercept the switching function (8), then instantaneously switching to $u = \mp u_0$.

The time required to complete the maneuver may be found by integrating the state equations along the optimal path to yield

$$t_f = \frac{I\dot{\theta}_0}{u_0}\operatorname{sgn}(s_0) + 2\sqrt{\frac{I}{u_0}\theta_0 \operatorname{sgn}(s_0) + \frac{1}{2}\left(\frac{I}{u_0}\dot{\theta}_0\right)^2} \tag{9}$$

Setting $\dot{\theta}_0 = 0$ gives the result for the "rest-to-rest" case:

$$t_f = 2\sqrt{\frac{I}{u_0}|\theta_0|} \tag{10}$$

The value of t_f found in Eq. (9) or (10) may be used as a starting point for any near-minimum time control law for a flexible structure. The degree to which the near-minimum time goal is achieved can be estimated by comparing the actual maneuver time with the idealized rigid-body time computed previously. However, this bang-bang control cannot be applied directly to a highly flexible system since the discontinuous nature of the control tends to excite the elastic modes.

Control Smoothing and Synthesis of the Feedback Control

The primary cause of excessive elastic-mode excitation in flexible spacecraft comes from abrupt control changes. If we assume that initially the flexible modes are quiescent, logically a control that excites them very little throughout the maneuver will enhance our ability to suppress them at the final time. Although the LQR control is nearly ideal in satisfying quiescent boundary conditions of controlled modes, it is less attractive for achieving near-minimum maneuver times. The final time must be specified, and there is no rigorous means by which the control magnitude constraints may be enforced. In addition, it requires real-time, perfect knowledge of modal coordinates, whereas in practice only a limited set of these may be estimated based on measurement of physical coordiantes. To achieve acceptable smoothness, u and $\dot{u}$ must be modeled as states with $\ddot{u}$ becoming the control.[10] Finally, Bryson's method[11] to enforce the terminal boundary conditions is computationally demanding, requiring the solution of $2n^2 + n$ differential equations for n modeled modes, thereby making modeling more than a very few flexible modes impractical.

We seek a feedback system that, while providing the essential smooth controls, approximates the characteristics of the minimum time control and is not computationally intensive. In any continuous momentum exchange system, actuator dynamics provide control smoothing to a certain degree, but this alone is insufficient for vibration suppression.

Smoothing Functions

Consider the approximation of the sgn function[13]:

$$\operatorname{sgn}(s) \approx \tanh\left(\frac{s}{1-\alpha}\right) \tag{11}$$

where $0 \le \alpha < 1$ is a smoothing function. Figure 2a illustrates the function for several values of α. As $\alpha \to 1$, the approximation of the sgn function becomes arbitrarily good. Also note that, unlike the sgn function, which is undefined at $s = 0$, the tanh function is continuous at all values of s. Alternatively, the arctangent function shows similar smoothing characteristics.[7,14] The tanh function is preferred here because it is easily represented in terms of exponential functions or series.

If we replace the sgn function in Eq. (7) with the tanh function in Eq. (11), we can realize any degree of smoothness desired for the control switch at $t = t_1$ and all subsequent interior switches. However, the initial jump discontinuity at $t = 0$ remains. This can be remedied by employing a multiplier function that ensures zero initial control magnitudes and control rates. Such a multiplier function is given by[15]

$$m(t) = \tau^2(3 - 2\tau), \qquad \tau = \begin{cases} t/T_1 & \text{for} \quad t \le T_1 \\ 1 & \text{for} \quad t > T_1 \end{cases} \tag{12}$$

where T_1 is "rise time," which can be selected to achieve whatever degree of control smoothness is desired. The profile of $m(t)$ is shown in Fig. 2b.

With these smoothing functions the control becomes

$$u = -u_0\left\{\tanh\left(\frac{s}{1-\alpha}\right)\right\}m(t) \tag{13}$$

The use of these smoothing functions, however, is not compatible with the switching function prescribed for the minimum time control in Eq. (8), which itself is discontinuous at the control switch. In addition, the smoothed control cannot follow the optimal trajectory because of the inherent lag in the control switch. We observe for the rigid-body rest-to-rest maneuver $t_1 = t_f/2$, from which it follows that the state-space trajectory is symmetric about the $\theta(t) = \theta_0/2$ line.

Variable Structure Control Systems

Variable structure control systems[16–21] change control laws along a switching line in order to drive the state-space trajectory to the phase-plane origin. Each control may, by itself, be unstable and, generally, the control is discontinuous at the switching line. Under certain conditions, once the state-space trajectory intercepts the switching line, the control switches at high frequency to cause it to chatter along the switching line to the origin.

The minimum time control system is a variable structure system where the control is discontinuously switched at the switching line $s = 0$ defined in Eq. (8). Now suppose that the parabolic switching line is replaced by a linear switching line of the form

$$s = \dot{\theta} + k\theta = 0 \tag{14}$$

Under certain ideal circumstances, the state-space trajectory will move along this switching line. The necessary conditions are

$$\lim_{s\to 0^-}, \qquad \dot{s} > 0 \tag{15a}$$

$$\lim_{s\to 0^+} \qquad \dot{s} < 0 \tag{15b}$$

The effect of Eqs. (15) is that, as the trajectory crosses the $s = 0$ line, the control changes sign and immediately forces it back toward the switching line. Ideally, control switching is instantaneous and the trajectory "slides" on the switching line to the origin. Hence, this is called the "sliding regime." In real systems, however, such infinite frequency switching is impossible and, instead, switching will occur at some high frequency determined by the limitation of the control mechanism. Slotine and Sastry[20] and Slotine[21] seek to avoid chattering via a multiplier function. The tanh function serves the same purpose with increased smoothness. When the conditions of Eqs. (15) are applied to Eqs. (6), (7), and (14), the following inequality results[18]:

$$I|\dot{\theta}|k < u_0 \Rightarrow k < \frac{u_0}{I|\dot{\theta}|} \tag{16}$$

That is, if $k > u_0/I|\dot{\theta}|$, regular switching occurs on or very near the switching line. Now define

$$k_{\max} = \frac{u_0}{I|\dot{\theta}|} \tag{17}$$

Replacing k with $k_{\max}$ in Eq. (14) gives

$$\theta + \frac{I}{u_0}\dot{\theta}|\dot{\theta}| = 0 \tag{18}$$

Thus, regular switching or sliding may be induced anywhere on the phase plane by selecting a switching function with the appropriate slope k at the point where switching is desired. To achieve near-minimum times for a maneuver, it is desirable that regular switching occur at $\theta_{\text{switch}} = \theta_0/2$, the control saturates, and the number of control switches is minimized. However, as the trajectory nears the origin, only small control inputs are necessary to correct any residual error.

The tanh function again proves to be useful; consider the switching line described by

$$s = \theta(t) + \frac{|\theta_{\text{switch}}|}{2}\left[\tanh\left(\frac{\dot{\theta}(t)+\varphi}{1-\beta}\right) + \tanh\left(\frac{\dot{\theta}(t)-\varphi}{1-\beta}\right)\right] \tag{19}$$

where β is a smoothing factor and φ a "deadband." Thus, the switching function in the state space is bounded by $\pm|\theta_{\text{switch}}|$ and passes through the origin. Note that it satisfies the two requirements that were placed on the desired switching line. The slope of the function in the state space is infinite at θ_{switch}, guaranteeing a regular switch as the trajectory crosses the $s = 0$ line. Near the origin, however, by selection of the appropriate values of β and φ, the slope can be made sufficiently small so that the state trajectory will track the switching line.

Smooth Control Law

At this point the smooth rest-to-rest maneuver can be assembled:

$$u = -u_0\left[\tanh\left(\frac{s}{1-\alpha}\right)\right]m(t) \tag{20}$$

$$s = \theta(t) + \frac{|\theta_{\text{switch}}|}{2}\left[\tanh\left(\frac{\dot{\theta}(t)-\varphi}{1-\beta}\right) + \tanh\left(\frac{\dot{\theta}(t)+\varphi}{1-\beta}\right)\right] \tag{21}$$

$$\theta_{\text{switch}} = \frac{\theta_0}{2} \tag{22}$$

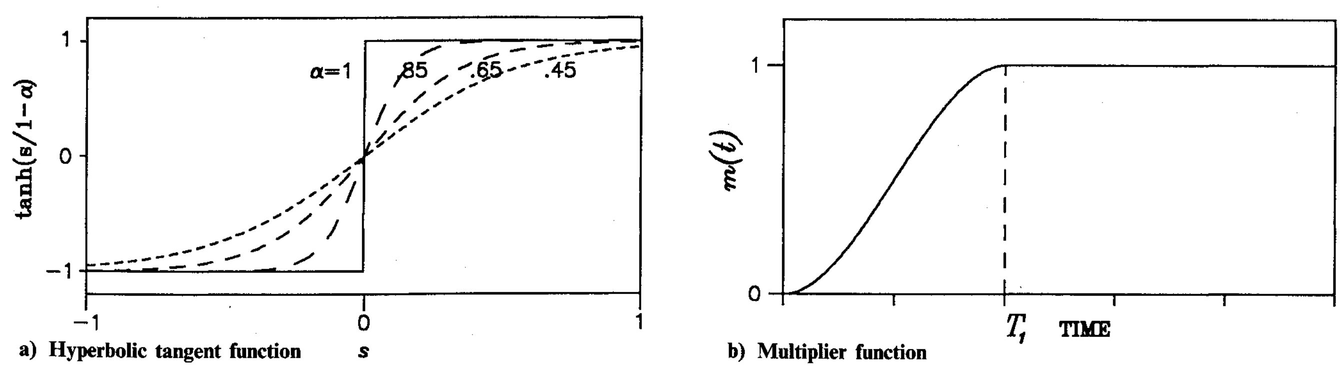

a) Hyperbolic tangent function b) Multiplier function

Fig. 2 Smoothing functions.

Example Maneuvers

The parameters α, β, φ, and T_1 provide an infinite variety of "user control" over the sharpness of control switches, while still preserving saturation constraints and the feedback nature of the control law. Figures 3 and 4 illustrate two possibilities for selection of values for these parameters. Figure 3 shows that a close approximation of the minimum time control is possible by choosing α and β close to 1, and T_1 small. The bang-bang control applied to a rigid spacecraft of equal moment of inertia is shown by the dashed line for comparison. Figure 4 compares the performance of the smooth control with relaxed values of α, β, and T_1 to that of a terminally constrained LQR control in which only the rigid-body mode and the first flexible mode of the spacecraft are measured and modeled. The maneuver time for the LQR was selected by trial such that the control just saturates.

Although symmetry of the state-space trajectory is not guaranteed, the feedback control law previously developed brings the rigid-body mode near the origin with final time unspecified. The control may reach, but not exceed, the saturation limit, and the energy of the flexible modes is dissipated via tracking a near-linear switching line at the end of the maneuver.

Especially noteworthy in this approach is the latitude that the designer has in choosing the degree of smoothness desired. T_1, α, β, and φ are all discretionary parameters. T_1 is the rise-time parameter that determines the smoothness of the initial control input. The value of α primarily affects the smoothness of the midmaneuver control switch, whereas β is the factor that controls the smoothness of the control near the origin. As $\beta \to 1$, the control transition will be rapid, but tracking along the switching line will be slow. As β decreases, the control transition will be smooth, and tracking of the switching line will be more rapid. However, if β is made too small, the trajectory may "overshoot" the origin. The deadband in the switching line, determined by φ, may be used to increase the slope of the switching line very near the origin to speed correction of residual error, while still allowing the value of β to stay relatively large. Although it is possible to have a similar deadband in the control itself, in general, little benefit has been found in such unless the system has a velocity constraint imposed. Since this is an undamped oscillatory system, the trajectory misses the target state by a small amount and must correct the error by tracking the switching line with very small control magnitudes. This is a shortcoming of this control law; it does not actively suppress flexible mode vibration until the end of the maneuver. Rather, it uses control smoothing to avoid exciting them. It is possible to use modal velocity feedback[22] to damp the critical flexible modes, but this increases the rigid-body mode maneuver time. Robustness can be inferred; extensive structural identification is unnecessary; only direct measurement of the rigid-body

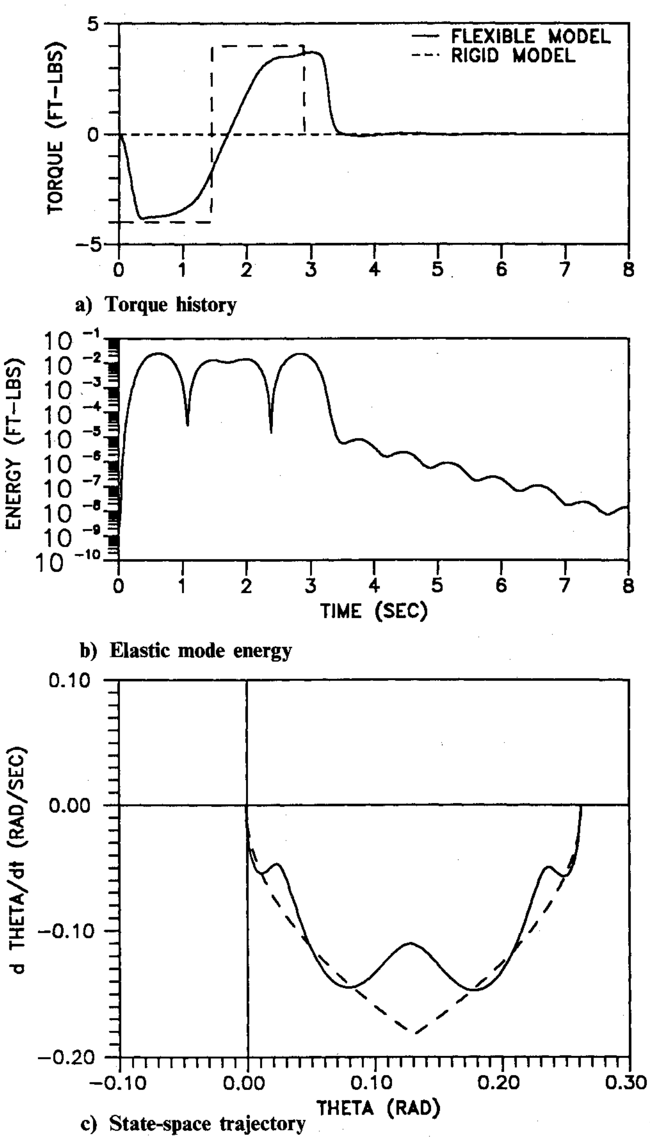

a) Torque history
b) Elastic mode energy
c) State-space trajectory

Fig. 3 15 deg rest-to-rest maneuver, $T_1 = 0.35$ s, $\alpha = 0.93$, $\beta = 0.97$.

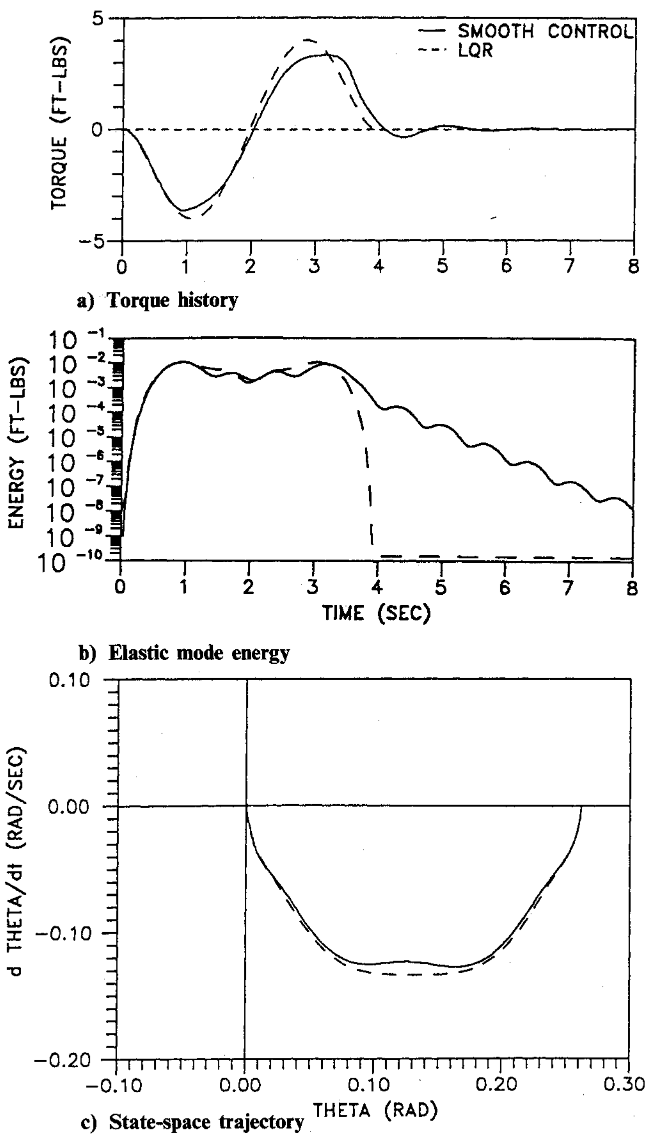

a) Torque history
b) Elastic mode energy
c) State-space trajectory

Fig. 4 15 deg rest-to-rest maneuver, $T_1 = 1.0$ s, $\alpha = \beta = 0.92$.

modes are considered. Moreover, although the smoothing parameters in the control law are affected by spacecraft parameters, e.g., moments of inertia, satisfactory values may be selected without accurate knowledge of the spacecraft structural data.

Target Tracking

The rest-to-rest maneuver, although important, is fairly restrictive. In many scenarios the target is moving with respect to the spacecraft, and it will be necessary not only to intercept its trajectory, but to subsequently track it. While examining the target tracking problem, it is convenient to adjust our notation to reflect the fact that the desired final state may not be stationary. Therefore, we define the relative error coordinate system

$$e = \theta - \theta_{\text{target}} \tag{23}$$

where θ_{target} is the rigid-body orientation of the target with respect to inertial frame whose origin is at the center of the spacecraft, and e is the relative "error" between the spacecraft rigid-body component and the target states.

From Eq. (23) it follows that

$$\dot{e} = \dot{\theta} - \dot{\theta}_{\text{target}} \tag{24}$$

$$\ddot{e} = \ddot{\theta} - \ddot{\theta}_{\text{target}} \tag{25}$$

which leads to the equations of motion for the rigid-body system:

$$I\ddot{e} = u - I\ddot{\theta}_{\text{target}} \tag{26}$$

Equation (26) suggests that it is possible to express the target acceleration as an equivalent control magnitude.

If maximum control effort is applied to a rigid body, its state-space trajectory describes a parabola. Along any given parabolic trajectory the relationship between $e(t)$ and $\dot{e}(t)$ remains constant; thus

$$e(t) = e_0 - \frac{I}{2u}[\dot{e}_0^2 - \dot{e}(t)^2] \tag{27}$$

where $u = \pm u_0$ as in Eq. (7). It is clear that it is possible to convert any "motion-to-rest" problem to an equivalent rest-to-rest problem by determining the value of $e(t)$ where the state-space trajectory intercepts the $\dot{e} = 0$ axis of the phase plane. Setting $\dot{e}(t) = 0$ in Eq. (27) and continuing the assumption that $u = \pm u_0$ gives

$$\hat{e}_0 = e_0 - \frac{I}{2u}\dot{e}_0^2 \tag{28}$$

with the regular switching angle defined:

$$e_{\text{switch}} = \frac{\hat{e}_0}{2} \tag{29}$$

The control law for the flexible spacecraft relies on the spacecraft approximately following these same trajectories. During $0 \le t \le T_1$, however, the flexible system does not exactly follow the ideal parabolic trajectory due to the presence of the multiplier function $m(t)$ given in Eq. (12) and the flexible characteristics of the spacecraft. If we assume that the initial state is sufficiently far from the would-be switching line so that the control would saturate if not constrained by $m(t)$, then the equation of motion (for a rigid system) for $0 \le t \le T_1$ is

$$I\ddot{e}(t)\,\mathrm{d}t = \frac{t^2}{T_1^2}\left(3 - 2\frac{t}{T_1}\right)u\,\mathrm{d}t \tag{30}$$

On integrating twice, we obtain

$$\dot{e}(T_1) = \dot{e}_0 + \frac{uT_1}{2I} \tag{31}$$

$$e(T_1) = e_0 + \dot{e}_0 T_1 + \frac{3uT_1^2}{20I} \tag{32}$$

After $t > T_1$, we assume that the control has saturated, and the trajectory is approximating the parabolic path. Therefore, we can revise our estimate of $\hat{e}_0$ by replacing e_0 and $\dot{e}_0$ in Eq. (31) with $e(T_1)$ and $\dot{e}(T_1)$ to give

$$\begin{aligned}\hat{e}_0 &= e(T_1) - \frac{I}{2u}\dot{e}(T_1)^2 \\ &= e_0 - \frac{I}{2u}\dot{e}_0^2 + \frac{T_1\dot{e}_0}{2} + \frac{u}{40I}T_1^2\end{aligned} \tag{33}$$

Target with Constant Angular Acceleration

We now consider the class of maneuvers in which a constant relative acceleration exists between the target state and the spacecraft. The motion-to-rest case, where a constant velocity difference initially exists, is a special case of this problem; relative acceleration between the target state and the spacecraft is zero. In Eq. (26) it was observed that, for the rigid-body system, the target acceleration could be expressed in terms of an equivalent control input by multiplying the target acceleration by the spacecraft axial moment of inertia. This allows us to reduce the problem to an equivalent motion-to-rest problem in which the control bounds are asymmetric about $u = 0$, i.e.,

$$u_{\min} \le u \le u_{\max}$$

$$u_{\min} = -u_0 - I\ddot{\theta}_{\text{target}}$$

$$u_{\max} = +u_0 - I\ddot{\theta}_{\text{target}}$$

Although $\ddot{\theta}_{\text{target}}$ is not directly measurable, it can be deduced from Eq. (25) and will hereinafter be expressed as $\ddot{\theta}_{\text{target}} = (\ddot{\theta} - \ddot{e})$.

Figure 5 portrays a representative maneuver for the rigid-body system in which the target and spacecraft states have a relative angular acceleration. Notice that the parabolic trajectories are not symmetric about the desired value of e_{switch}.

The equation for the equivalent rest-to-rest initial angle is expressed in terms of $u = \pm u_0$, the sign of which, ironically, is

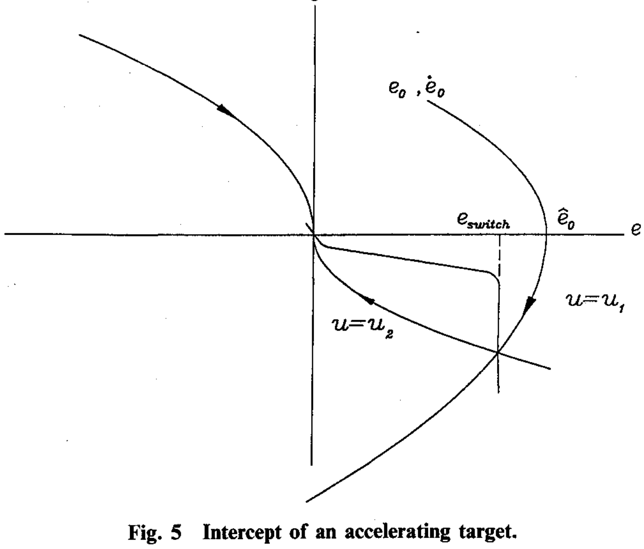

Fig. 5 Intercept of an accelerating target.

dependent on the initial conditions. We cannot determine the value of s upon which the switching logic depends until $\hat{e}_0$ and e_{switch} are calculated. But these cannot be calculated without knowing sgn(s). A sign convention is established by recalling the parabolic switching function in Eq. (8), which can now be written

$$s_p = e(t) + \frac{I}{2|u|}\dot{e}(t)|\dot{e}(t)| = 0 \tag{34}$$

This curve represents the optimal switchless trajectories to the origin and is constant regardless of initial conditions. All that is needed is the value of $s_p(t=0) \equiv s_{p_0}$. Thus

$$s_{p_0} = e_0 + \frac{I}{2|u|}\dot{e}_0|\dot{e}_0| \tag{35}$$

Replacing u with the appropriate control magnitude gives

$$s_{p_0} = e_0 + \frac{I\dot{e}_0|\dot{e}_0|}{2[u_0 + I(\ddot{\theta} - \ddot{e})\ \mathrm{sgn}(\dot{e}_0)]} \tag{36}$$

Recalling Eq. (33) and assuming that $T_1 < t_1$ (where t_1 is the time to the control switch)

$$\hat{e}_0 = e_0 + \frac{T_1}{2}\dot{e}_0 + \frac{I\dot{e}_0^2}{2[u_0\,\mathrm{sgn}(s_{p_0}) + I(\ddot{\theta} - \ddot{e})]} - \frac{[u_0\,\mathrm{sgn}(s_{p_0}) + I(\ddot{\theta} - \ddot{e})]T_1^2}{40I} \tag{37}$$

Now the asymmetric control bounds may be defined as

$$u(t) = \begin{cases} u_1, & 0 \le t < t_1 \\ u_2, & t_1 \le t \le t_f \end{cases} \tag{38}$$

where

$$u_1 = -u_0\,\mathrm{sgn}(s_{p_0}) - I(\ddot{\theta} - \ddot{e}) \tag{39a}$$

$$u_2 = u_0\,\mathrm{sgn}(s_{p_0}) - I(\ddot{\theta} - \ddot{e}) \tag{39b}$$

Thus, the trajectory for $0 \le t < t_1$ may be described by

$$e(t) = \hat{e}_0 + \frac{I}{2u_1}\dot{e}(t)^2 \tag{40}$$

and the trajectory for $t_1 \le t \le t_f$ is

$$e(t) = \frac{I}{2u_2}\dot{e}(t)^2 \tag{41}$$

Equating Eqs. (40) and (41) gives

$$\dot{e}^2_{\text{switch}} = \frac{2\hat{e}_0}{I}\left(\frac{u_1 u_2}{u_1 - u_2}\right) \tag{42}$$

Substituting Eq. (42) into Eq. (41) gives

$$\begin{aligned} e_{\text{switch}} &= \hat{e}_0\left(\frac{u_1}{u_1 - u_2}\right) \\ &= \frac{\hat{e}_0}{2}\left[\frac{u_0\,\mathrm{sgn}(s_{p_0}) + I(\ddot{\theta} - \ddot{e})}{u_0\,\mathrm{sgn}(s_{p_0})}\right] \\ &= \frac{\hat{e}_0}{2}\left[\frac{u_0 + I(\ddot{\theta} - \ddot{e})\ \mathrm{sgn}(s_{p_0})}{u_0}\right] \end{aligned} \tag{43}$$

The major characteristic that distinguishes the constant acceleration case from the previous cases is the fact that, although the relative states go to the origin as before, the control does not go to zero. Once the target state is intercepted, continued control effort, $u = I(\ddot{\theta} - \ddot{e})$, is necessary to keep the target and spacecraft states coincidental. Thus, it is necessary to rewrite Eq. (20):

$$u = [-u_0 + I(\ddot{\theta} - \ddot{e})\ \mathrm{sgn}(s)]\left[\tanh\left(\frac{s}{1-\alpha}\right)\right]m(t) + I(\theta - \ddot{e})m(t) \tag{44}$$

Inspection of Eq. (44) reveals that when s is sufficiently large to saturate the control, $|u| = u_0$, and as $s \to 0$ near the origin, $u = I(\ddot{\theta} - \ddot{e})$, which is the behavior we desire. Unfortunately, with this control the sign of $u(t)$ does not change at $e(t) = e_{\text{switch}}$ as desired. Instead, the control actually changes sign where

$$[u_0 + I(\ddot{\theta} - \ddot{e})\ \mathrm{sgn}(s)]\left[\tanh\left(\frac{s}{1-\alpha}\right)\right] = I(\ddot{\theta} - \ddot{e}) \tag{45}$$

Solving for s we find that the control switches at

$$s_{\text{switch}} = \left(\frac{1-\alpha}{2}\right)\ell n\left\{\frac{u_0 + I(\ddot{\theta} - \ddot{e})[\mathrm{sgn}(s) + 1]}{u_0 + I(\ddot{\theta} - \ddot{e})[\mathrm{sgn}(s) - 1]}\right\} \tag{46}$$

Thus, in order to have the control switch as desired,

$$e_{\text{switch}} = \frac{\hat{e}_0}{2}\left[\frac{u_0 + I(\ddot{\theta} - \ddot{e})\ \mathrm{sgn}(s_{p0})}{u_0}\right] - s_{\text{switch}}\left[\frac{u_0 - I(\ddot{\theta} - \ddot{e})\ \mathrm{sgn}(s_{p0})}{u_0}\right] \tag{47}$$

Equations (21), (44), (46), and (47) give a complete set of equations for controlling the spacecraft to track a target state with constant angular acceleration. They are, in fact, compatible with all previous maneuvers considered.

A representative maneuver is shown in Fig. 6. As one might expect from a near-minimum time maneuver, except for the influence of control smoothing, the control is saturated until target interception. Subsequently, the control becomes a tracking control. Although postrendezvous energy appears high, it is manifest as potential strain energy as a result of continued control input to sustain tracking. Modal kinetic energy is very small, In fact, if the control in Eq. (20) is substituted for that in Eq. (44), the control would still attempt to track the target state. However, a steady-state error results. This steady-state error is found to be

$$e(\infty) = \frac{1-\alpha}{2}\ell n\left(\frac{u_0 - I(\ddot{\theta} - \ddot{e})}{u_0 + I(\ddot{\theta} - \ddot{e})}\right) \tag{48}$$

The accelerating target case illustrates a major advantage of this control design over the alternate approaches to quiescent boundary conditions such as the LQR. With only a minor modification of the control law, a target with an acceleration component can be intercepted with a control profile that possesses the characteristics of a minimum time control; the control saturates, and there is only a single control switch until the time very near the interception. No additional constraints beyond the kinematic constraints $e(t_f) = \dot{e}(t_f) = 0$ need be included.

Multibody/Multiactuator Configurations

The control technique thus far developed is not restricted to single-actuator, single-body systems. It can also be applied to multiple, interconnected bodies with multiple controls. As a general illustration of the techniques required, consider the generic two-body system in Fig. 7. This is an approximate model of the Rapid Retargeting and Precision Pointing (R2P2) experiment being conducted by Martin Marietta Corp. The dynamical system consists of two bodies: A is rigid, while B is flexible. The actual dimensions of the R2P2 model are proprietary, but it is significantly larger, and the flexible

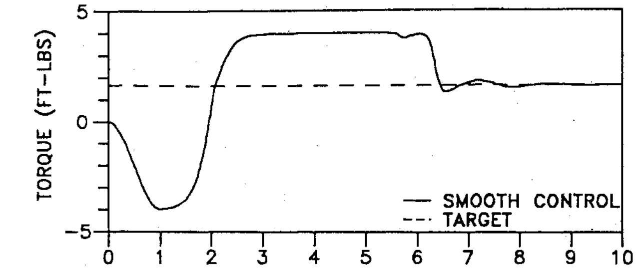

a) **Torque history**

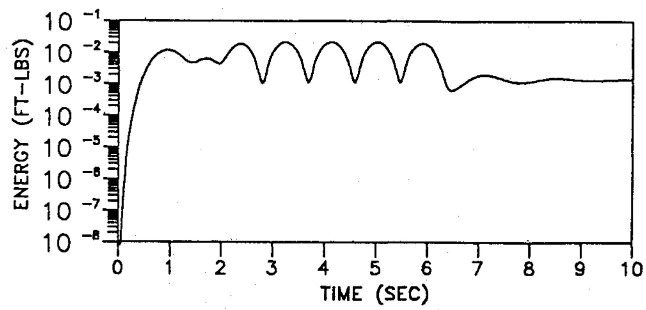

b) **Elastic mode energy**

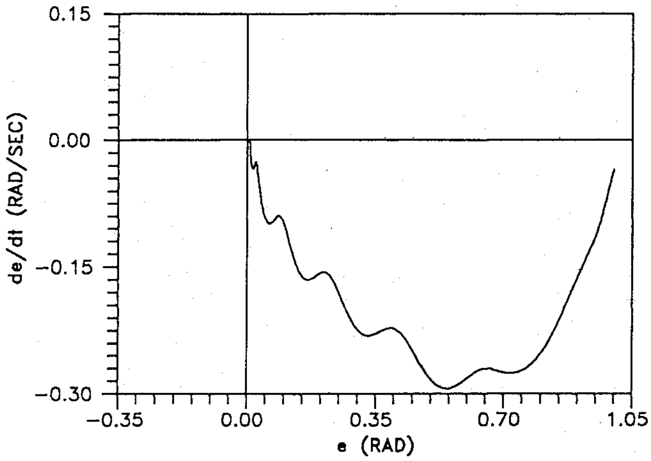

c) **State-space trajectory**

Fig. 6 Accelerating target intercept maneuver, $e_0 = -57.3$ deg, $\dot{e}_0 = 2$ deg/s, $\ddot{\theta}_{\text{target}} = 5$ deg/s^2

body B is qualitatively more rigid than the system heretofore considered. Body A has a continuous momentum exchange-type actuator. In addition, an active joint ("gimbalflex") actuator, which generates the torque U_B and the F_y parallel to the y axis, is required to prevent large lateral displacements between the two rotating bodies.

In developing the control for the multibody system, we will proceed as before, first evaluating the rigid-body dynamics and then smoothing the control for application to the flexible system.

After linearization, the equations of motion for the system may be expressed in matrix form[23]:

$$\begin{Bmatrix} \ddot{\theta} \\ \ddot{\phi} \\ \ddot{Y} \end{Bmatrix} = \begin{bmatrix} \dfrac{R_B}{I_B} & 0 & \dfrac{-1}{I_B} \\ \left(\dfrac{R_B}{I_B} - \dfrac{R_A}{I_A}\right) & \dfrac{1}{I_A} & -\left(\dfrac{1}{I_A} + \dfrac{1}{I_B}\right) \\ \left(\dfrac{1}{m_A} + \dfrac{1}{m_B} + \dfrac{R_A^2}{I_A} + \dfrac{R_B^2}{I_B}\right) & \dfrac{-R_A}{I_A} & \left(\dfrac{R_A}{I_A} - \dfrac{R_B}{I_B}\right) \end{bmatrix} \begin{Bmatrix} F_y \\ U_A \\ U_B \end{Bmatrix} \tag{49}$$

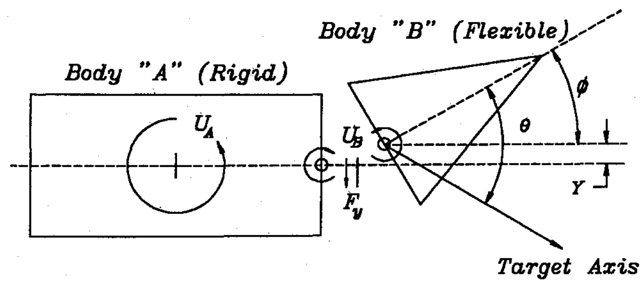

Fig. 7 Multiple-body/actuator system.

where $m_{A,B}$ are the body masses, $R_{A,B}$ the moment arms from the mass centers to the interface, and $I_{A,B}$ the moments of inertia about the centroidal axis of each body, respectively. In Eq. (49), for simplicity, we ignore all flexible-body effects. We have, in other developments, included flexible-body effects (of body B), and the simulated controlled responses discussed below include flexible-body effects.

The net control torque on A and B is

$$\begin{aligned} U_{A_{\text{net}}} &= U_A - U_B - R_A F_y \\ U_{B_{\text{net}}} &= U_B - R_B F_y \end{aligned} \tag{50}$$

Two scenarios are examined. In the first, it is desired to rotate the entire system in a synchronized manner, so that ϕ, the angle between the two bodies, is kept as small as possible. In the second scenario, it is desired to rotate only the flexible portion of the system, leaving the rigid-body orientation undisturbed. In both cases, the major task is ascertaining the permissible control limits for each actuator.

It is clear that the permissible torque to ensure synchronization may not coincide with the actual physical limits of the actuators. Generally, the physical limits of one of the actuators will constrain the remainder to some less than maximum limit. In addition, it is possible that the system may have acceleration or velocity limits that do not permit the full exploitation of the actuators. Here, we allow U_A to saturate and find new control limits for U_B, and F_y to satisfy the constraints.

Setting $\ddot{\phi} = 0$ in Eq. (49) and substituting Eq. (50) gives

$$\frac{U_{A_{\text{net}}}}{U_{B_{\text{net}}}} = \frac{I_A}{I_B} \tag{51}$$

This result is confirmed by equating the maneuver times for each body from Eq. (10). Now setting $\ddot{Y} = 0$ in Eq. (49) to ensure that the displacement between A and B remains small, and substituting with Eqs. (50) and (51) gives

$$F_y = \frac{(R_A + R_B) m_A m_B}{I_A (m_A + m_B)} U_{A_{\text{net}}} \tag{52}$$

Let the saturation torque of U_A be U_{A_0}. From Eqs. (50) and (52)

$$|U_{A_{\text{net}\,0}}| = \frac{U_{A_0} I_A (m_A + m_B)}{(I_A + I_B)(m_A + m_B) + (R_A + R_B)^2 m_A m_B} \tag{53}$$

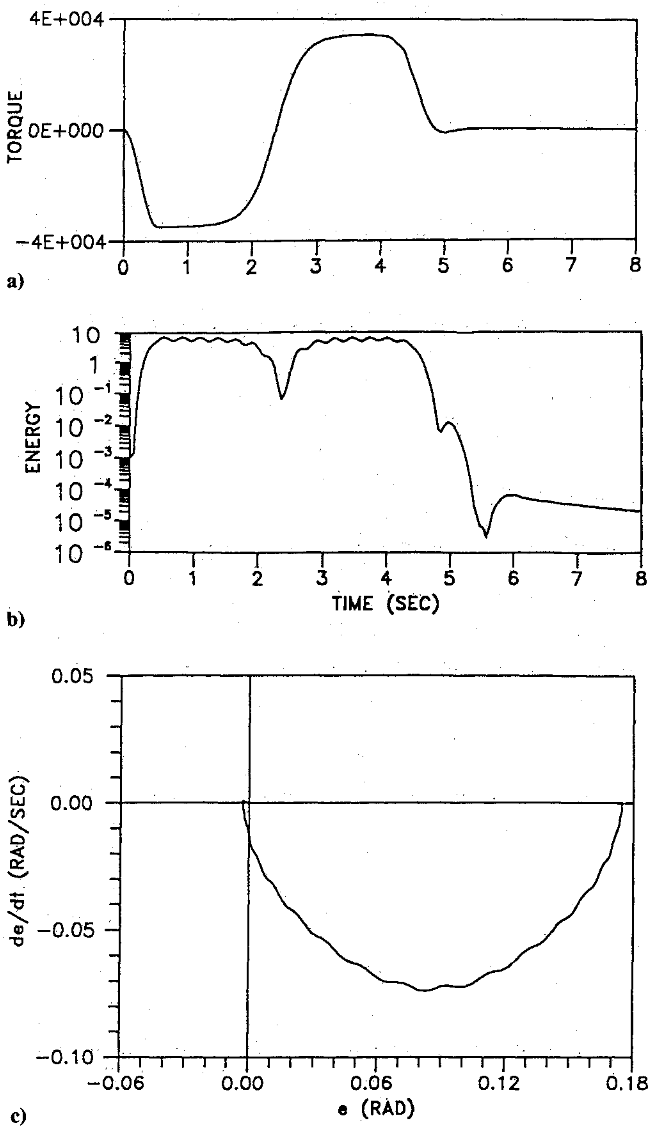

Fig. 8 10 deg rest-to-rest maneuver.

F_{y_0} is now found from Eq. (52) and

$$U_{B_0} = \frac{I_B}{I_A} U_{A_{\text{net}\,0}} + R_B F_{y_0} \tag{54}$$

In the second case under consideration, it is desired to rotate the flexible body as rapidly as possible while leaving the rigid body's orientation undisturbed. Setting $\ddot\theta = \ddot\phi$ in Eq. (49) leads to the logical outcome that $U_{A_{\text{net}}} = 0$. Now the flexible-body actuator is the limiting factor; the control torque necessary to prevent A from rotating will be small compared to the actuator limits. Setting $\ddot Y = 0$ gives

$$F_y = \frac{R_B m_A m_B U_B}{I_B m_B + I_B m_A + R_B^2 m_A m_B} \tag{55}$$

and, from Eq. (50), with $U_{A_{\text{net}}} = 0$:

$$U_A = U_B + R_A F_y \tag{56}$$

If an initial displacement $Y(0) = Y_0 > 0$ exists, $\ddot Y = 0$ will result in a linear displacement in time between the two bodies. To compensate for this a damping term is introduced, via

$$\ddot Y = -2\zeta\omega_n \dot Y - \omega_n^2 Y = d \tag{57}$$

where ω_n is selected to be some cutoff frequency appropriate to the structure, and $\zeta = 1$. Equations (52) and (55) are used to calculate control limit F_{y_0} after which d (which is expected to be very small) is added to time-varying value of F_y from those equations.

It is clear that in both scenarios the saturation limits of the controls are related by constant ratios. Once the control limits for the particular maneuver are established, it is a simple matter to apply them to the smoothing functions found previously. The control histories of the three actuators differ only in magnitude. Figure 8 shows the control of the flexible portion (body B) of the two-body spacecraft for a synchronized maneuver, including the rotational/vibrational coupling effects that cause the high-frequency effects evident in Figs. 8b and 8c. The high-frequency effects are much more pronounced for sharper control histories.

Conclusions

The problem of slewing a flexible spacecraft in near-minimum time has been considered. A relatively simple control scheme was developed by approximating the minimum time bang-bang control for a rigid body. The control law was modified to accommodate accelerating targets by converting the problem to an equivalent rest-to-rest maneuver with asymmetric control bounds. It was shown that it can be applied to systems with multiple bodies and actuators. Simulations using models of both very flexible and nearly rigid structures verify that this approach is workable for a wide range of space structures.

Sufficient control smoothing and symmetry of the state-space trajectory about the control switch are the most important factors in ensuring that the flexible modes of vibration are quiescent in the least time for rest-to-rest maneuvers. Of lesser importance is the smoothness of the initial and terminal control.

This control design is simple and can be executed in real time; it is very robust and unaffected by spacecraft parameter estimation error. Final time is not specified and state estimation is not required.

Acknowledgments

This research was made possible by funding provided by the U.S. Air Force Office of Scientific Research Contract F49620-86-K-00014DEF, under Dr. Anthony Amos, and Martin Marietta (Denver) Aerospace Contract GH-180166, with technical monitor Dr. Gary Skidmore. We are grateful for their support. Furthermore, we wish to acknowledge the invaluable assistance we received from A. M. Browder and Dr. R. C. Thompson. We value their friendship and encouragment as much as their technical expertise.

References

[1]Junkins, J. L. and Turner, J. D., *Optimal Spacecraft Rotational Maneuvers*, 1st ed., Elsevier, New York, 1985.

[2]Turner, J. D. and Junkins, J. L., "Optimal Large-Angle Single-Axis Rotational Maneuvers of Flexible Spacecraft," *Journal of Guidance and Control*, Vol. 4, Nov.–Dec. 1980, pp. 578–585.

[3]Turner, J. D. and Chun, H. M., "Optimal Distributed Control of a Flexible Spacecraft Using Control-Rate Penalties in the Controller Design," AIAA/AAS Astrodynamics Conf., San Diego, CA, Aug. 1982.

[4]Juang, J. N., "Frequency-Shaped Large-Angle Maneuvers," AIAA Paper 87-0174, Jan. 1987.

[5]Vander Velde, W. and He, J., "Design of Space Structure Control Using On-Off Thrusters," *Journal of Guidance, Control, and Dynamics*, Vol. 6, Jan.–Feb. 1983, pp. 53–60.

[6]Floyd, M. A., "Single Step Optimal Control of Large Space Structures, Doctor of Science Thesis, Massachusetts Inst. of Technology, Cambridge, MA, 1984.

[7]Singh, G., Kabamba, P. T., and McClamroch, N. H., "Planar Time Optimal, Rest to Rest, Slewing Maneuvers of Flexible Spacecraft," *Journal of Guidance, Control, and Dynamics*, Vol. 12, Jan.–Feb. 1989, pp. 71–81.

[8]Thompson, R. C., Junkins, J. L., and Vadali, S. R., "Near Minimum Time Open Loop Control of Dyanmic Systems," AIAA Paper 87-0958, April 1987.

[9]Breakwell, J. A., "Optimal Feedback Slewing of Flexible Spacecraft," *Journal of Guidance and Control*, Vol. 4, Sept.–Oct. 1981, pp. 472–479.

[10]Junkins, J. L., "Comment on 'Optimal Feedback Slewing of Flexible Spacecraft'," *Journal of Guidance and Control*, Vol. 5, May–June 1982, pp. 318.

[11]Bryson, A. E., Jr., and Ho, Y.-C., *Applied Optimal Control*, rev. printing, Hemisphere, Washington, DC, 1975, pp. 158–167.

[12]Ryan, E. P., *Optimal Relay and Saturating Control System Synthesis*, 1st ed., Peter Perigrinus, Ltd., London, 1982.

[13]Wang, P. K. C., "Control of Distributed Parameter Systems," *Advances in Control Systems*, edited by C. T. Leondes, Academic, New York, 1964, pp. 75–172.

[14]Subrahmanyam, M. B., "Computation of Optimal Controls by Newton's Method Using a Discretized Jacobian," *Journal of Guidance, Control, and Dynamics*, Vol. 9, May–June 1986, pp. 371–374.

[15]Vadali, S. R. and Junkins, J. L., "Optimal Open-Loop and Stable Feedback Control of Rigid Spacecraft Attitude Maneuvers," *Journal of Astronautical Sciences*, Vol. 32, No. 2, April–June 1984, pp. 105–122.

[16]Itkis, U., *Control Systems of Variable Structure*, 1st ed., Wiley, New York, 1976.

[17]Öz, H. and Özunger, Ü., "Variable Structure System Control for Flexible Spacecraft," AIAA Paper 84-2002, Aug. 1984.

[18]Vadali, S. R., "Variable Structure Control of Spacecraft Large-Angle Maneuvers," *Journal of Guidance, Control, and Dynamics*, Vol. 9, March–April, 1986, pp. 235–239.

[19]Mostafa, O. and Öz, H., "Maneuvering of Flexible Spacecraft Via VSC," AIAA/AAS Guidance, Navigation, and Control Conf., Williamsburg, VA, Aug. 1986.

[20]Slotine, J. J. and Sastry, S. S., "Tracking Control of Non-Linear Systems Using Sliding Surfaces with Applications to Robot Manipulators," *International Journal of Control*, Vol. 38, Feb. 1983, pp. 465–492.

[21]Slotine, J. J., "Sliding Controller Design for Non-linear Systems," *International Journal of Control*, Vol. 40, No. 2, 1984, pp. 421–434.

[22]Balas, M. J., "Direct Velocity Feedback Control of Large Space Structures," *Journal of Guidance and Control*, Vol. 2, May–June 1979, pp. 252–253.

[23]Browder, A. M., Junkins, J. L., Vadali, S. R., and Ward, D. T., "Control Methodologies for Space Based Laser Rapid Retargeting and Precision Pointing," Final Rept., Texas A&M Univ., College Station, TX, Martin Marietta Denver Aerospace Contract GH6-180166, Jan. 1988.

[24]Byers, R. M., "Feedback Control Design for Smooth, Near Minimum time Rotational Maneuvers of Flexible Spacecraft," M.S. Thesis, Texas A&M Univ., College Station, TX, Aug. 1987.